Dynamic scaling relation in quantum many-body systems

Devendra Singh Bhakuni and Yevgeny Bar Lev*
Department of Physics, Ben-Gurion University of the Negev, Beer-Sheva 84105, Israel

(Received 19 September 2023; accepted 28 June 2024; published 10 July 2024)

In delocalized systems, particle number fluctuations, also known as quantum surface roughness, and the mean-square displacement exhibit a temporal power law growth followed by a saturation to a system size–dependent value. We use simple scaling arguments to show that these quantities satisfy the Family-Vicsek scaling law and derive a dynamic scaling relation between the dynamical exponents, assuming that the saturation times of both quantities scale similarly with the system size. This relation clarifies the mechanism behind quantum surface roughness growth and suggests that diffusive quantum many-body systems belong to the Edwards-Wilkinson universality class. Moreover, it provides a convenient way to assess quantum transport in cold-atoms experiments. We numerically verify our results by studying two noninteracting models and one interacting model having regimes with distinct dynamical exponents.

DOI: 10.1103/PhysRevB.110.014203

I. INTRODUCTION

In the vicinity of a continuous phase transition, many physical properties of a system exhibit a power law dependence, manifested by critical exponents [1–3]. Scaling arguments show that the critical exponents are not independent but related via scaling relations [2,3]. Moreover, renormalization group theory explains why microscopically different physical systems, which belong to the same universality class, share the same critical exponents [1,3–6]. While the concepts of scaling and universality were originally introduced for systems at equilibrium, they were successfully generalized to classical out-of-equilibrium systems [7–20]. One of the prominent examples of dynamical scaling occurs in classical surface physics [8–10]. Surface roughness of a surface segment of length L is defined as the standard deviation of surface height. It typically increases as a power law in time before saturating to a value which depends on the surface segment length, following the famous Family-Vicsek (FV) scaling [9,10],

$$w(L,t) = L^{\alpha} f(t/L^{z}), \tag{1}$$

where $f(x)$ is a unitless function which for $t \ll L^z$ grows as $f(x) \sim x^{\beta}$ and for $t \gg L^z$ saturates to a constant independent of L. The exponents α and β are the roughening and growth exponents, respectively, and the exponent z, called a dynamical exponent, defines the saturation time, $t_{\text{sat}} \sim L^z$. Since the early time growth of $w(L,t)$ does not depend on the system size, from the properties of $f(x)$, it follows that the exponents satisfy the dynamic scaling relation $z = \alpha/\beta$. Well-known universality classes in one-dimensional classical systems are the Kardar-Parisi-Zhang (KPZ) [12] class with $\alpha = 1/2$ and $\beta = 1/3$ and the Edwards-Wilkinson (EW) class with $\alpha = 1/2$ and $\beta = 1/4$ [8]. In higher dimensions, the solution of the EW equation suggests $\alpha, \beta \leqslant 0$ [8,21], whereas numerical studies have shown logarithmic growth [22–25]. The KPZ class in higher dimensions was also studied numerically [26,27]. These classes have found application in a wide variety of physical systems such as sedimentation of colloidal particles [28], growth of bacterial colonies [29], fire fronts [30,31], spin chains [32–36], and driven-dissipative condensates [37–39].

Quite recently, the notion of surface roughness was generalized to quantum systems [40–42]. Using an analogy between the fluctuating hydrodynamics and stochastic surface growth, the *quantum surface height* was defined as the number of particles in a finite domain such that the quantum surface roughness corresponds to the particle number fluctuations [43–46]. For delocalized noninteracting fermions, the surface roughness was shown to follow FV scaling with the exponents $\alpha = 1/2$ and $\beta = 1/2$, which was called a ballistic class [40]. In contrast, in the localized phase, the FV scaling is not satisfied due to suppression of roughness growth. It was argued that generic delocalized systems will feature $\alpha = 1/2$, whereas for systems with a mixture of localized and delocalized states, they were shown to have $\alpha,\ \beta \neq 1/2$ [40]. The question of what determines the growth exponent β is, however, still largely open.

Another prominent dynamical quantity which shows power law growth is the spreading of density excitation of conserved quantities. In delocalized systems, the spreading is typically governed by a power law with dynamical exponent, β_{tr}, followed by a saturation to a system size–dependent value. For single-particle systems, this dynamical exponent is known to be related to the fractal dimension of the single-particle eigenstates [47–50]. In this article, we establish a dynamic scaling relation between the growth exponent of the surface roughness, or analogously, the particle number fluctuations, and the dynamical exponent characterizing transport of a corresponding conserve quantity. We demonstrate the relationship by numerically studying two noninteracting models with tunable transport regimes: the one-dimensional Fibonacci chain and the three-dimensional Anderson model. Furthermore, we

*Contact author: ybarlev@bgu.ac.il

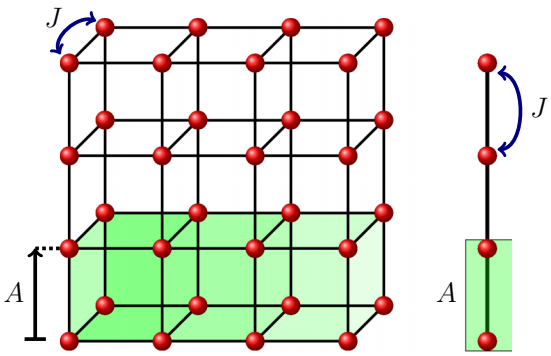

FIG. 1. Schematic of the domain in three dimensions (left) and in one dimension (right) used to calculate the surface roughness.

show that such a relationship also holds for an interacting system.

II. SURFACE ROUGHNESS AND PARTICLE FLUCTUATIONS

The total number of particles (fermions or bosons) in a finite connected domain A of a d-dimensional lattice is

$$\hat{N}_A = \sum_{i\in A} \hat{n}_i(t), \tag{2}$$

where $\hat{n}_j$ is the particle number operator on site $\boldsymbol{j}$. We note that up to an insignificant constant, this corresponds to the *quantum* surface height operator as defined in Refs. [40,41] (see Appendix A). We will designate the quantum expectation of the number of particles as $\langle \hat{N}_A(t)\rangle = \mathrm{Tr}[\hat{\rho}(t)\hat{N}_A]$, where $\hat{\rho}(t)$ is the density matrix of the system at time t.

The fluctuations of the particle number in domain A are given by

$$\Delta N_A(t) = \sqrt{\langle \hat{N}_A^2(t)\rangle - \langle \hat{N}_A(t)\rangle^2}. \tag{3}$$

Without loss of generality, we will focus on a rectangular domain A which corresponds to a half of the system (Fig. 1). We assume that the total number of particles is conserved, and the continuity equation ensures that the change in N_A and ΔN_A is proportional to the surface area, $|\partial A| = L^{d-1}$, of domain A. In analogy to the classical surface roughness, whose early time behavior does not depend on the dimensions of domain A, we normalize the particle fluctuations,

$$w(L,t) = \Delta N_A(t)/L^{(d-1)/2}, \tag{4}$$

such that it corresponds to the definition of the quantum surface roughness, extended to an arbitrary dimension (see Refs. [40,41] and Appendix A). Here, L is the linear dimension of the system, and for our choice of A, it is also the linear dimension of A.

For one-dimensional delocalized systems, $w(L,t)$ follows the FV scaling [Eq. (1)] with roughening exponent $\alpha = 1/2$ and a growth exponent β which is system dependent [40,41]. In what follows, we show that this is also true in higher dimensions. For thermalizing systems, initial states with sufficiently high energy density have exponentially decaying correlations between the positions of the particles. Neglecting those correlations all together, which is exact in the infinite temperature state, yields $w_\infty(L,t) \sim L^{1/2}$, for any particle density and dimension (see Appendix A). Comparing with (1), this corresponds to $\alpha = 1/2$. For *classical,* noninteracting diffusive systems, the particle fluctuations (3) grow as $t^{1/4}$ such that $\beta = 1/4$ [51–53].

III. SPREADING OF EXCITATIONS AND DYNAMICAL SCALING RELATION

Transport of conserved quantities at temperature T can be characterized by the density-density correlation function,

$$C_i(t) = \langle (\hat{n}_i(t) - \langle \hat{n}_i\rangle)(\hat{n}_{i_0}(0) - \langle \hat{n}_{i_0}\rangle)\rangle, \tag{5}$$

where the expectation $\langle \hat{O}\rangle$ is taken with respect to the finite temperature density matrix, $\hat{\rho}_T$, such that $\langle \hat{n}_i(t)\rangle \equiv \mathrm{Tr}\hat{\rho}_T\hat{n}_i(t)$. The correlation function describes the spreading of a density excitation at site $\boldsymbol{i}_0$ of a d-dimensional lattice [54–57]. The width of this excitation, also called the mean-square displacement (MSD), is given by

$$R^2(t) = \sum_i |\boldsymbol{i} - \boldsymbol{i}_0|^2 C_i(t). \tag{6}$$

For delocalized systems, the MSD grows as $t^{\beta_{\mathrm{tr}}}$ with the exponent β_{tr} characterizing the transport. For example, $\beta_{\mathrm{tr}} = 1$ corresponds to diffusion, whereas $\beta_{\mathrm{tr}} = 2$ corresponds to ballistic transport.

We argue that similar to the surface roughness or the particle fluctuations, the MSD also follows FV scaling, with a growth exponent β_{tr}. We define delocalized systems as a system where an initial density excitation spreads uniformly over the system such that the MSD saturates to L^2. Therefore, for delocalized systems, $\alpha_{\mathrm{tr}} = 2$, and $z_{\mathrm{tr}} = \alpha_{\mathrm{tr}}/\beta_{\mathrm{tr}} = 2/\beta_{\mathrm{tr}}$. From the continuity equation, the change in the number of particles in domain A is related to the integrated current density in this domain [58]. This means that the fluctuations in the number of particles are related to the fluctuations of the integrated current. The integrated current is a local observable, which is connected to a conserved quantity. As such, its fluctuations will saturate on the time scale it takes for a density perturbation to traverse the subsystem. Given the preceding, we conjecture that the saturation of the particle number fluctuation occurs on the same time scale it takes for a local density excitation to become uniform, $L^{z_{\mathrm{tr}}}$. This implies that $z = z_{\mathrm{tr}}$, and since, as argued earier, $\alpha = 1/2$ and $\alpha_{\mathrm{tr}} = 2$, it yields the dynamic scaling relation, $\beta = \beta_{\mathrm{tr}}/4$, which constitutes the main result of this work. This relation is consistent with Ref. [40], which found $\beta = 1/4$ for a delocalized system with $\beta_{\mathrm{tr}} = 2$. In what follows, we numerically verify this relation for one-dimensional and three-dimensional noninteracting systems featuring *distinct* transport regimes, β_{tr}. We also provide evidence that this relation holds in a one-dimensional *interacting* system.

IV. NONINTERACTING SYSTEMS

We consider a system of noninteracting particles moving in an external potential with the Hamiltonian,

$$\hat{H} = -\sum_{\langle \boldsymbol{n},\boldsymbol{m}\rangle} J(\hat{a}_{\boldsymbol{n}}^\dagger \hat{a}_{\boldsymbol{m}} + \hat{a}_{\boldsymbol{m}}^\dagger \hat{a}_{\boldsymbol{n}}) + \sum_{\boldsymbol{n}} W_{\boldsymbol{n}} \hat{a}_{\boldsymbol{n}}^\dagger \hat{a}_{\boldsymbol{n}}. \tag{7}$$

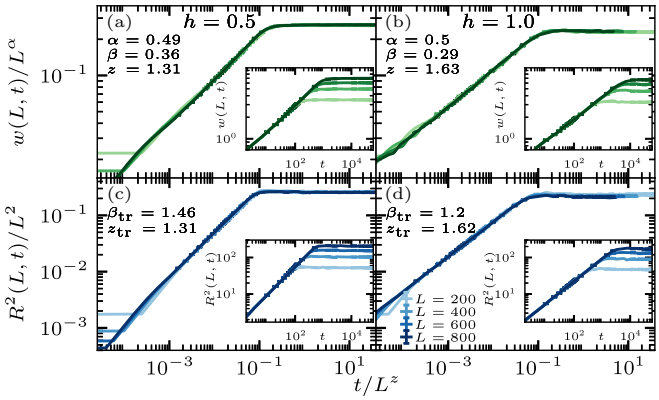

FIG. 2. Dynamical scaling of the surface roughness (top row) and the MSD (bottom row) for the Fibonacci chain with $h = 0.5, 1$. The inset shows the data without the rescaling. System sizes used for the simulation are $L = 200$–800.

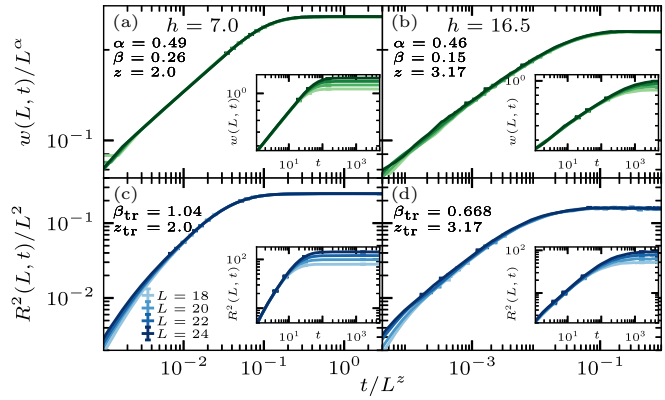

FIG. 3. Same as Fig. 2 but for the three-dimensional Anderson model at the delocalized ($h = 7$) and critical ($h = 16.5$) phases. The linear dimension of the system sizes we simulated are $L = 18$–24.

Here, $\hat{a}_{\boldsymbol{n}}, \hat{a}^{\dagger}_{\boldsymbol{n}}$ annihilate and create a fermion at site $\boldsymbol{n}$ on a d-dimensional lattice; J is the hopping strength, which without loss of generality, we set $J = 1$; and $\langle . \rangle$ designates nearest-neighbor sites. The external potential is given by $W_{\boldsymbol{n}}$. We focus on two specific systems: a one-dimensional Fibonacci chain of length L and a three-dimensional Anderson model on a cubical lattice with side L. For the Fibonacci chain, the on-site potential is given by $W_n = h(2g(bn) - 1)$, with h being the strength of the potential and $g(x) = [x + b] - [x]$, where $[x]$ denotes the integer part of x and $b = \frac{1}{2}(\sqrt{5} - 1)$ is the golden mean. The Fibonacci model exhibits multifractal single-particle states for *any* value of the potential strength [59–63]. Transport is known to cross over from ballistic transport ($\beta_{\rm tr} = 2$) at $h = 0$ to subdiffusive transport ($\beta_{\rm tr} < 1$) for large h [64–68]. For the Anderson model in three dimensions, the on-site potential is uniformly drawn from the interval $W_{\boldsymbol{n}} \in [-h/2, h/2]$, where h corresponds to the strength of the disorder. The delocalized phase of the Anderson model is diffusive ($\beta_{\rm tr} = 1$), and anomalous transport ($\beta_{\rm tr} = 2/3$) and multifractal eigenstates exist only at the critical point, $h = 16.5J$ [49,69–71]. We average the quantities of interest over 50 independent disorder realizations for the Anderson model and over *50* samples of the Fibonacci sequence for the Fibonacci chain [72].

To maximize the growth of the surface roughness, we initiate the system from states with a definite number of particles in domain A, which we chose to be half of the system (see Fig. 1). For the Fibonacci chain, we evolve the system starting from a charge-density-wave state, $|\psi_{\rm 1D}\rangle = \prod_{i=1}^{L/2} \hat{a}^{\dagger}_{2i}|0\rangle$, and for the three-dimensional Anderson model, we use the checkerboard pattern, $|\psi_{\rm 3D}\rangle = \prod_{\rm mod(i+j+k,2)=0} \hat{a}^{\dagger}_{i,j,k}|0\rangle$. Here, $|0\rangle$ denotes the vacuum and (i, j, k) correspond to a point on a cubical lattice in three dimensions. The energy of these states is close to the middle of the many-body spectrum, and therefore, for delocalized dynamics, we expect the surface roughness to approach the infinite temperature limit. The surface roughness is calculated after numerically evolving the single-particle density matrix. This matrix is dense and and has L^{2d} elements, and therefore, for the three-dimensional Anderson problem, we are limited to a linear dimension of about $L = 24$.

The insets of Figs. 2(a) and 2(b) show the dynamics of the surface roughness for the Fibonacci model for a set of parameters $h = 0.5, 1.0$, and a range of system sizes $L = 200$–800, whereas the insets of Figs. 3(a) and 3(b) show a similar plot for the three-dimensional Anderson model for the delocalized ($h = 7$) and critical ($h = 16.5$) phases, and for a linear dimension of $L = 18$–24. The surface roughness grows as a power law in time and saturates to a system size–dependent value. The data for different system sizes can be collapsed into a single curve by rescaling $w(L, t)$ and t by L^{α} and L^{z}, respectively [see the main panels of Figs. 2(a), 2(b) and 3(a), 3(b)], which suggests the existence of FV scaling. We perform the scaling collapse by minimizing the deviation $\chi(\alpha, z) = \sum_{L,t} |w(L_0, t) - (L/L_0)^{-\alpha} w(L, (L/L_0)^{z} t)|/w^2(L_0, t)$, with L_0 being a reference system size, which allows us to extract the exponents α and β [41,73] (see Appendix D for the z exponents). Figure 4 shows the calculated exponents for both systems as a function of the external potential. For all values of the external potential, $\alpha \approx 1/2$ and β is monotonously decreasing from a

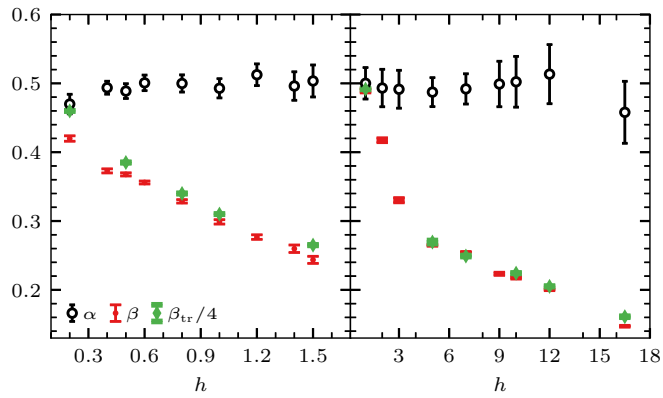

FIG. 4. The open black circles correspond to the α exponent, and the full red circles to the β exponent of the surface roughness as a function of the potential strength h. The left panel is the Fibonacci chain, and the right column is the three-dimensional Anderson model. The green diamonds correspond to $\beta_{\rm tr}/4$, where $\beta_{\rm tr}$ is the transport exponent as computed from the MSD.

ballistic value ($\beta = 1/2$). Interestingly, contrary to the predictions of the classical EW equation in three dimensions predicts ($\alpha, \beta < 0$) [8,21], we find that the quantum surface roughness exhibits exponents similar to that of the one-dimensional case. The localized phase does not show FV scaling since the surface roughness saturates to a value which does not depend on the system size (data not shown). We now proceed showing that the MSD also follows the FV scaling and that the dynamical scaling relation, $\beta = \beta_{\rm tr}/4$, holds.

We numerically obtain the MSD by propagating the correlation function (5), which for noninteracting systems amounts to evolving a vector of length L^d. As such, much larger system sizes are accessible compared to the surface roughness. Since the initial charge-density-wave initial conditions we use for the surface roughness correspond to an energy density in the middle of the many-body spectrum, we compute the correlation function at infinite temperate. In Figs. 2(c), 2(d) and 3(c), 3(d), we show that similarly to the surface roughness, the MSD follows FV scaling with the exponents $\alpha_{\rm tr} = 2$ and $\beta_{\rm tr}$. Figure 4 shows a remarkable agreement between $\beta_{\rm tr}/4$ and β for both the Fibonacci chain and the three-dimensional Anderson models for all studied strengths of the potential, verifying the dynamic scaling relation. For both models, the $\beta_{\rm tr}/4$ is monotonically decreasing from a ballistic value for very weak disorder ($\beta_{\rm tr}/4 = 1/2$) to subdiffusive values ($\beta_{\rm tr}/4 < 1/4$) for higher-potential strengths. We note that for the three-dimensional Anderson model, diffusion is expected ($\beta_{\rm tr}/4 = 1/4$) for $h < h_c = 16.5$. However, its numerical observation requires $l \ll L$, where l is the mean-free path. Since $l \sim h^{-2}$, large systems sizes are required to observe the asymptotic transport for weak external potential (see Appendix C for finite size analysis). Interestingly, even outside the asymptotic transport regime, the relationship between $\beta_{\rm tr}$ and β is satisfied.

V. INTERACTING SYSTEM

To verify if the dynamic scaling relationship holds in the presence of interactions, we consider an interacting Fibonacci chain with the nearest-neighbor interaction

$$\hat{H}_{\rm int} = V \sum_i (\hat{n}_i - 1/2)(\hat{n}_{i+1} - 1/2), \tag{8}$$

where V is the interaction strength. We focus on potential strengths for which the system is ergodic [67,68,74]. For the interacting case, the numerical complexity is exponential in the system size such that we are limited to $L = 24$ sites. Due to the limited power law growth regime, it is hard to reliably extract β and $\beta_{\rm tr}$ for such system sizes (see Appendix C for finite size analysis). Instead, in Fig. 5, we compare the root MSD $R(t)$ to the square of the surface roughness $w^2(L,t)$. If the dynamic relation, $\beta = \beta_{\rm tr}/4$, holds, these quantities are supposed to be proportional up to a constant dependent on the potential strength. In Fig. 5, we see that this is indeed the case: both quantities have the same growth exponent, yet the surface roughness takes more time to reach saturation. While we focus on half-filling here, we show in Appendix E that such a relation also holds away from the half-fillings as well.

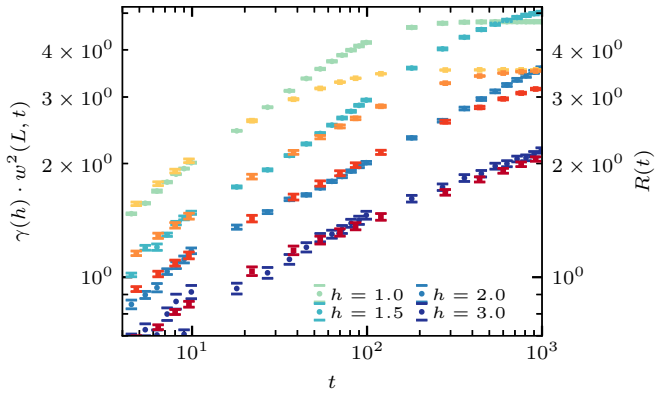

FIG. 5. The square of surface roughness, $w^2(L,t)$ (blue points), and root MSD, $R(t)$ (red squares), as a function of time and a number of potential strengths for the interacting Fibonacci chain with parameters $L = 24$, $V = 1.0$. More intense colors correspond to larger potential strength. The surface roughness is multiplied by a disordered dependent factor $\gamma(h)$ to obtain a visual match with $R(t)$ at early times.

VI. DISCUSSION

In this article, we conjecture that MSD follows FV scaling and saturates on the same time scale as the surface roughness or, analogously, particle number fluctuations. Using this conjecture, we obtain a dynamic relationship between the transport exponent and the growth exponent of the surface roughness, $\beta = \beta_{\rm tr}/4$, which applies to any particle density. We numerically confirm this conjecture by studying two prototypical noninteracting quantum systems in one and three dimensions, and one interacting system in one dimension, where transport can be controlled by the strength of the external potential. While we numerically confirm the dynamical relationship in fermionic systems, since our argument does not depend on the statistics of the particles, we expect it to also hold for bosonic systems.

It is important to note that for *classical diffusive and noninteracting* systems, a connection between particle fluctuations and transport can be derived using fluctuating hydrodynamics, which puts diffusive systems in the EW ($\beta = 1/4$) universality class [51–53]. However, for simple *interacting* cases, such as the symmetric exclusion process, this relation does *not* hold [58,75–77]. Moreover, there is no known relationship between these quantities for *classical* systems with *anomalous* transport. On the contrary, our results suggest that for *quantum* systems, the dynamic scaling relationship holds also for anomalous transport and interacting systems. We argue that the difference between classical and quantum cases follows due to indistinguishability between the particles in quantum dynamics, which allows collective relaxation of the density even in one-dimensional systems, where classical dynamics exhibit single-file motion. In higher dimensions, we expect that the dynamical scaling relation will hold also for classical interacting systems.

The established dynamic scaling relationship explains the mechanism behind the quantum surface roughness growth, and provides a convenient way to assess transport in cold-atoms experiments, where particle number fluctuations can be

directly measured. Indeed, while our work was in preparation, this method was used in a recent cold-atoms experiment [78].

Our study leaves a number of questions open. For noninteracting systems, the transport exponent is related to the multifractal properties of the single-particles states [47–49] (see also Appendix D). Is there a similar relationship for the interacting system? Can one derive a formal connection between surface roughness growth and transport? Is the dynamic relation sensitive to the energy density of the initial state? And how does the universality class change when the system is coupled with a dissipative environment?

During the final stages of preparation of this article, a related and complementary study appeared [79].

ACKNOWLEDGMENTS

We would like to thank Naftali Smith for fruitful discussions. This research was supported by a grant from the United States–Israel Binational Foundation (BSF, Grant No. 2019644), Jerusalem, Israel; the United States National Science Foundation (NSF, Grant No. DMR-1936006); and by the Israel Science Foundation (Grants No. 527/19, 218/19, and 1304/23). D.S.B. acknowledges funding from the Kreitman Fellowship.

APPENDIX A: PARTICLE NUMBER FLUCTUATIONS AND SURFACE ROUGHNESS

Particle numbers in domain A are defined in Eq. (2) in the main text,

$$\hat{N}_A = \sum_{i\in A} \hat{n}_i(t), \tag{A1}$$

which can be contrasted to the height operator defined in Refs. [40,41],

$$\hat{h}_A = \sum_{i\in A} (\hat{n}_i(t) - \nu) = \hat{N}_A - \nu V_A,$$

where $\nu = N/V$ is the particle density and V_A is the number of sites in domain A. Since νV_A is a constant, the fluctuations in $\hat{N}_A$ coincide with the surface roughness – the fluctuations of the height operator.

At infinite temperature the average number of particles in domain A is

$$\langle \hat{N}_A \rangle_\infty = \sum_{i\in A} \langle \hat{n}_i \rangle_\infty = \nu V_A. \tag{A2}$$

Similarly, the square of the number of particles is

$$\begin{aligned}\langle \hat{N}_A^2 \rangle_\infty &= \sum_{i\in A}\sum_{j\in A} \langle \hat{n}_i \hat{n}_j \rangle_\infty = \sum_{i\in A} \langle \hat{n}_i^2 \rangle_\infty + \sum_{i\neq j\in A} \langle \hat{n}_i \hat{n}_j \rangle_\infty \\ &= \sum_{i\in A} \langle \hat{n}_i^2 \rangle_\infty + \sum_{i\neq j\in A} \langle \hat{n}_i \rangle \langle \hat{n}_j \rangle_\infty = \alpha_\nu V_A + \nu^2 V_A (V_A - 1),\end{aligned} \tag{A3}$$

where $\alpha_\nu \equiv \langle \hat{n}_i^2 \rangle$ is a constant which is ν for fermions and $\nu(1+\nu)$ for bosons. To simplify the calculation of $\langle \hat{n}_i \hat{n}_j \rangle$, we have used the grand-canonical ensemble, where $\langle \hat{n}_i \hat{n}_j \rangle_\infty = \langle \hat{n}_i \rangle \langle \hat{n}_j \rangle_\infty$ for $i \neq j$. Therefore, the fluctuations at infinite temperature are given by

$$\begin{aligned}\Delta N_A &= \sqrt{\langle \hat{N}_A^2 \rangle_\infty - \langle \hat{N}_A \rangle_\infty^2} = \sqrt{(\alpha_\nu - \nu^2) V_A} \\ &= \begin{cases} \sqrt{\nu(1-\nu) V_A} & \text{fermions} \\ \sqrt{\nu V_A} & \text{bosons} \end{cases}.\end{aligned} \tag{A4}$$

For a domain half the size of the system, $V_A = L^d/2$ and, therefore,

$$\langle \hat{N}_A \rangle_\infty \sim L^d \Delta N_A \sim L^{d/2} w_\infty(L,t) \sim L^{d/2-(d-1)/2} = L^{1/2}. \tag{A5}$$

A similar calculation can be performed also for a fixed number of particles with a canonical ensemble. To leading order in $1/V$, it gives

$$\langle \hat{n}_i \hat{n}_j \rangle = \tfrac{1}{4} - \tfrac{1}{4V}, \tag{A6}$$

which yields a subleading, and therefore insignificant, correction to $w_\infty(L,t)$.

APPENDIX B: DYNAMICS OF ENTANGLEMENT ENTROPY

For a subsystem described by a reduced density matrix $\rho_s(t)$, the dynamics of the entanglement entropy can be calculated as $S(L,t) = -\mathrm{Tr}[\rho_s(t)\ln\rho_s(t)]$, which for the free fermionic case is related to the eigenvalues c_α of the two-point correlation function $\langle \hat{a}_i^\dagger(t)\hat{a}_j(t)\rangle$ restricted to the subsystem [80,81],

$$S(L,t) = -\sum_i [c_\alpha \log c_\alpha + (1-c_\alpha)\log(1-c_\alpha)]. \tag{B1}$$

For noninteracting systems, the entanglement entropy is related to the surface roughness or the particle number fluctuations in the subsystem as $S(L,t) \propto w^2(L,t)$ [40,82]. Thus, the dynamics of the entanglement entropy is also expected to follow the FV scaling with the modified exponents $(2\alpha, 2\beta, z)$.

We plot the dynamics of the half-chain entanglement entropy in Fig. 6 for the noninteracting Fibonacci chain for potential strengths $h = 0.5,\ 1.0$, and for system sizes $L =$ 200–800. Similar to the surface roughness, the entanglement entropy grows in a power law fashion followed by a system size–dependent saturation [insets of Figs. 6(d)–6(f)]. Performing a rescaling of $S(L,t)$ and t by $L^{2\alpha}$ and L^z, respectively,

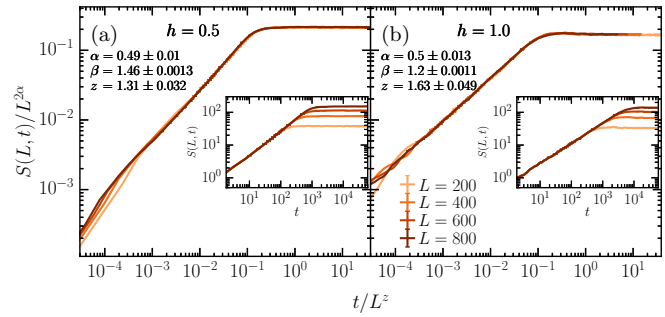

FIG. 6. Dynamical scaling of the entanglement entropy for the Fibonacci chain with $h = 0.5,\ 1$. The inset shows the data without the rescaling. System sizes used for the simulation are $L =$ 200–800.

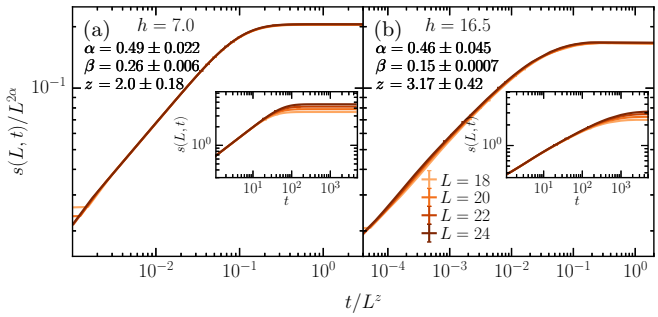

FIG. 7. Same as Fig. 6 but for the three-dimensional Anderson model at the delocalized ($h = 7$) and critical ($h = 16.5$) phases. The linear dimensions of the system sizes we simulated are $L = 18$–24.

we see a collapse of the data for different L to a single curve (Fig. 6) which suggest the presence of FV scaling in the entanglement entropy.

Similarly, for the three-dimensional Anderson model, the entanglement entropy normalized by the area, $s \equiv S/L^2$, is plotted in Fig. 7 for disorder strengths $h = 7,\ 16.5$ and linear dimensions $L = 18$–24. We consider the subsystem to be one half of the cube and the normalization to remove the dependence of the system size on the initial dynamics. Similarly to the one-dimensional Fibonacci chain, we see the presence of FV scaling in the entanglement entropy for the three-dimensional Anderson model with the exponents $(2\alpha, 2\beta, z)$. For the interacting case, the relationship between the particle number number fluctuation and entanglement entropy does not hold anymore and the exponents $(2\alpha, 2\beta, z)$ are no longer expected. However, particle number fluctuations present a lower bound on the entanglement entropy such that $\beta_{\text{ent}} > \beta$ [82,83]. We confirm this by studying the dynamics of the entanglement entropy for the interacting Fibonacci chain. We plot the dynamics of the entanglement entropy for the system size $L = 24$ and a range of potential strengths $h = 1.0 - 3.0$ in Fig. 8. Similarly to the surface roughness and the RMSD, we see that the entanglement entropy grows as a power law in time followed by a saturation. A comparison with the square of the surface roughness/particle number fluctuations $w^2(L,t)$ is also provided in Fig. 8. In contrast to the noninteracting

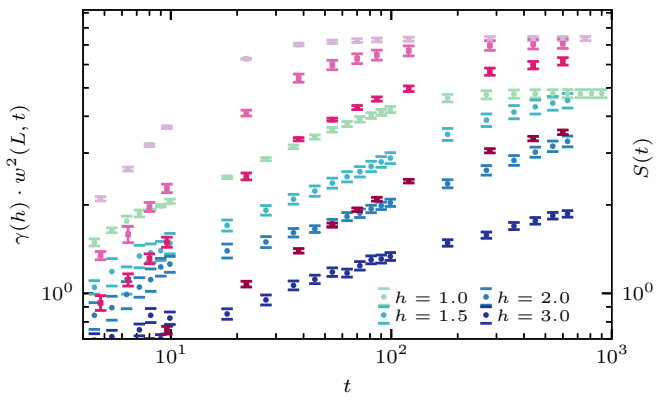

FIG. 8. Dynamics of entanglement entropy (red squares) for the interacting Fibonacci chain for $L = 24$. The square of surface roughness (blue points), $w^2(L,t)$, is also plotted for a comparison.

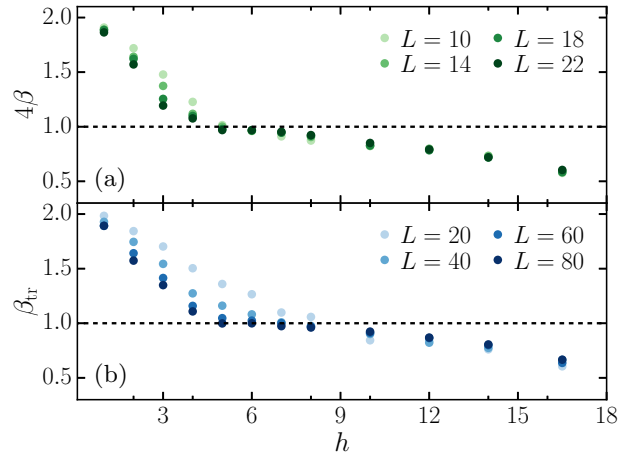

FIG. 9. Finite size analysis for the three-dimensional Anderson model. The top panel is the growth exponent for $L = 14$–22. The bottom panel is for transport growth for $L = 20$–80. The flow toward the EW class is clearly visible in the delocalized side. The dashed line corresponds to the diffusive transport with $\beta_{\text{tr}} = 1$.

case, the entanglement entropy grows faster than $w^2(L,t)$ and the relationship $\beta_{\text{ent}} = 2\beta$ does not hold anymore.

APPENDIX C: FINITE SIZE ANALYSIS

In Fig. 9, we plot the surface roughness exponent β and the transport exponent β_{tr} for the three-dimensional Anderson model, as a function of the potential strength h system sizes $L = 14$–22. The surface roughness exponent is multiplied by a factor of 4 to match with the transport exponent. It can be seen that for all disorder strengths, the relationship between the exponents $\beta_{\text{tr}} = 4\beta$ holds. Furthermore, for disorder smaller than the critical disorder strength ($h < h_c = 16.5$), we see that both 4β and β_{tr} approach to 1 (marked by a dashed line) as the system size increases and signifies diffusive transport. These growth exponents suggest an EW universality class for quantum diffusive systems.

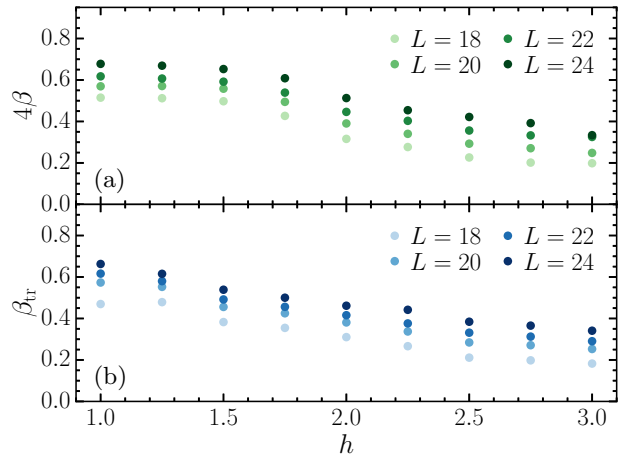

FIG. 10. Similar to Fig. 9 but for the interacting Fibonacci chain with $V = 1.0$. The system sizes are $L = 18$–24.

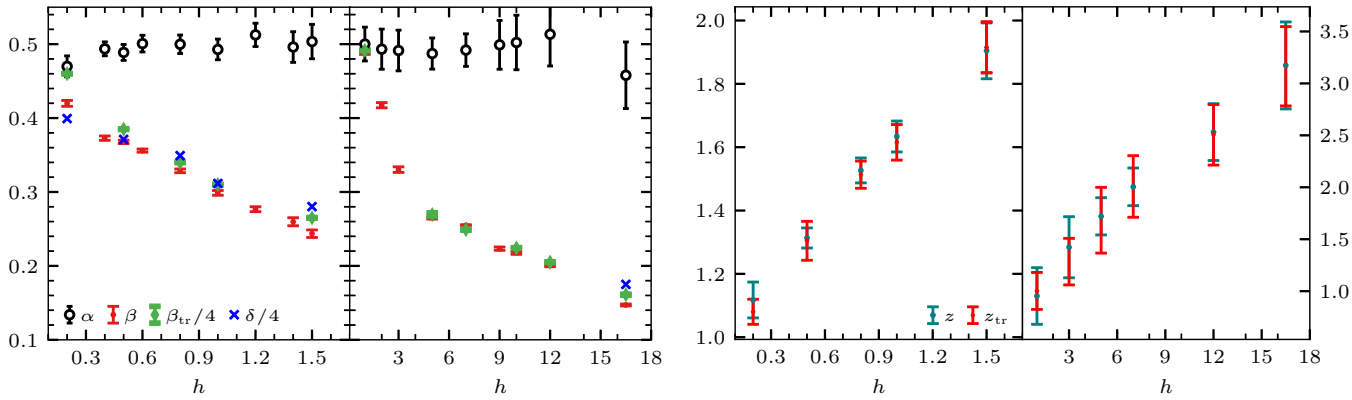

FIG. 11. Left: Dynamic exponents of the surface roughness α (open black circles), β (red circles) and transport exponent $\beta_{\rm tr}$ (green diamonds) as a function of the potential strength h for the Fibonacci chain (left) and the three-dimensional Anderson model (right). The black crosses correspond to $\delta/4$, where $\delta = D_2^{\mu}/D_2^{\psi}$. Right: Dynamical exponents z (circles) and $z_{\rm tr}$ (diamonds) as a function of h for Fibonacci and three-dimensional Anderson models.

In Fig. 10, we present a similar analysis for the interacting Fibonacci chain for interaction strength $V = 1$ and system sizes $L = 18$–24. Similar to the non-interacting case, we see that the relationship between the transport exponent $\beta_{\rm tr}$and the surface roughness/particle fluctuations exponent β holds ($\beta_{\rm tr} = 4\beta$).

APPENDIX D: MULTIFRACTALITY AND DYNAMICAL EXPONENTS

Eigenstates of quantum systems often exhibit self-similar (multi)fractal behavior in the vicinity of a quantum phase transition [71,84–90]. Such states are spatially extended but sparse, and are characterized by (multi)fractal dimensions. A celebrated example of multifractal eigenstates occurs at the critical point of the three-dimensional Anderson model [71,91–96]. Other notable examples are the ground state of quantum Hall systems [85,87], quasiperiodic systems [97–100], long-range systems [101–104], and random regular graphs [105]. Using the previously established connection between transport in noninteracting systems and (multi)fractality of single-particle eigenstates [47–49], we argue that the surface growth exponent is also related to (multi)fractal properties.

For noninteracting systems, the dynamical exponent of the MSD growth $\beta_{\rm tr}$ is related to the fractal dimensions, $\delta = D_2^{\mu}/D_2^{\psi}$ [47–49]. Here, D_2^{μ} is the correlation dimension of the local density of states and D_2^{ψ} is the correlation dimension of the single-particle eigenstates. Since we have shown that the transport exponent is related to the surface roughness growth exponent as $\beta = \beta_{\rm tr}/4$, using the relationship $\beta_{\rm tr} = \delta = D_2^{\mu}/D_2^{\psi}$ we obtain $\beta \simeq \delta/4$. We verify this relation for both the Fibonacci and Anderson models by plotting β and $\delta/4$ for various values of h (see Fig. 11) using the values of D_2^{μ} and D_2^{ψ} from Refs. [47–49].

APPENDIX E: DYNAMICS AWAY FROM HALF-FILLING

In this section, we study the dynamics of the particle number fluctuations and the transport away from the half-filling. We specifically focus on the interacting case and perform the same analysis presented in Fig. 5 but with filling factors

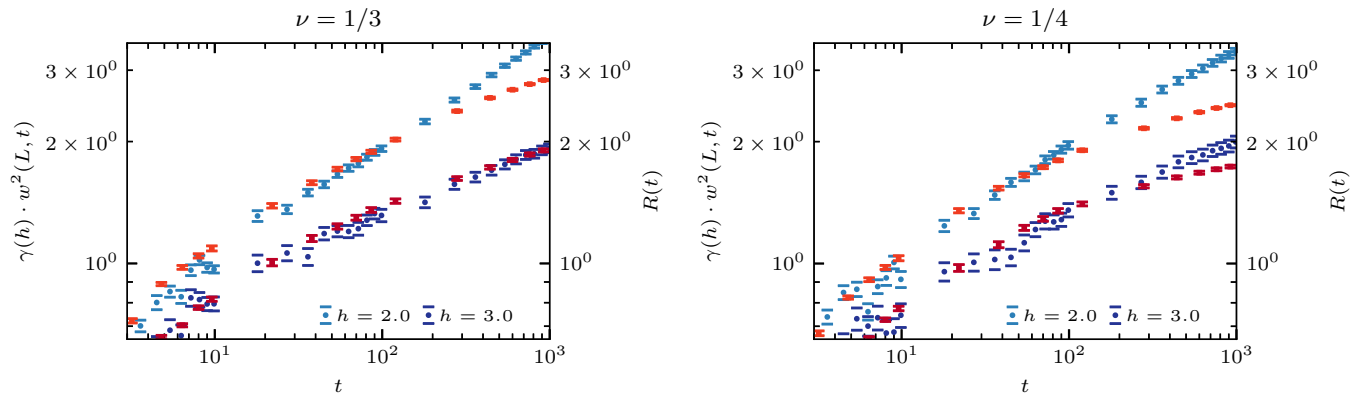

FIG. 12. The square of surface roughness, $w^2(L,t)$ (blue points), and root MSD, $R(t)$ (red squares), as a function of time and for different potential strengths for the interacting Fibonacci chain with parameters $L = 24$, $V = 1.0$ and filling factors $\nu = 1/3$ (left), $\nu = 1/4$ (right). More intense colors correspond to larger potential strength. The surface roughness is multiplied by a disordered dependent factor $\gamma(h)$ to obtain a visual match with $R(t)$ at early times.

$\nu = 1/3$ and $\nu = 1/4$ respectively for a system size $L = 24$ (Fig. 12). Similar to the half-filling case, we see that the relationship between the dynamical exponents also holds away from the half-filling.

[1] H. E. Stanley, *Phase Transitions and Critical Phenomena* (Clarendon Press, Oxford, 1971), Vol. 7.

[2] J. Zinn-Justin, *Quantum Field Theory and Critical Phenomena*, 4th ed., International Series of Monographs on Physics Vol. 113 (Clarendon Press, Oxford, 2002).

[3] G. Ódor, Rev. Mod. Phys. **76**, 663 (2004).

[4] C.-L. Hung, X. Zhang, N. Gemelke, and C. Chin, Nature (London) **470**, 236 (2011).

[5] A. Lesne and M. Lagües, *Scale Invariance: From Phase Transitions to Turbulence* (Springer, Berlin, 2012).

[6] S. V. Andreev, A. A. Varlamov, and A. V. Kavokin, Phys. Rev. Lett. **112**, 036401 (2014).

[7] S. R. Broadbent and J. M. Hammersley, Math. Proc. Camb. Philos. Soc. **53**, 629 (1957).

[8] S. F. Edwards and D. R. Wilkinson, Proc. Roy. Soc. Lond. Ser. A **381**, 17 (1982).

[9] T. Vicsek and F. Family, Phys. Rev. Lett. **52**, 1669 (1984).

[10] F. Family and T. Vicsek, J. Phys. A: Math. Gen. **18**, L75 (1985).

[11] W. Kinzel, Z. Phys. B **58**, 229 (1985).

[12] M. Kardar, G. Parisi, and Y.-C. Zhang, Phys. Rev. Lett. **56**, 889 (1986).

[13] A.-L. Barabási and H. E. Stanley, *Fractal Concepts in Surface Growth* (Cambridge University Press, Cambridge, 1995).

[14] A. Bray, Adv. Phys. **43**, 357 (1994).

[15] T. Halpin-Healy and Y.-C. Zhang, Phys. Rep. **254**, 215 (1995).

[16] J. Krug, Adv. Phys. **46**, 139 (1997).

[17] H. Hinrichsen, Adv. Phys. **49**, 815 (2000).

[18] K. A. Takeuchi, M. Sano, T. Sasamoto, and H. Spohn, Sci. Rep. **1**, 34 (2011).

[19] K. A. Takeuchi and M. Sano, Phys. Rev. Lett. **104**, 230601 (2010).

[20] I. Corwin, Notices Amer. Math. Soc. **63**, 230 (2016).

[21] T. Nattermann and L.-H. Tang, Phys. Rev. A **45**, 7156 (1992).

[22] S. Pal, D. P. Landau, and K. Binder, Phys. Rev. E **68**, 021601 (2003).

[23] S. Pal and D. Landau, Physica A **267**, 406 (1999).

[24] M. Plischke, Z. Rácz, and D. Liu, Phys. Rev. B **35**, 3485 (1987).

[25] W. Kwak and J. M. Kim, Physica A **520**, 87 (2019).

[26] T. J. Oliveira, S. G. Alves, and S. C. Ferreira, Phys. Rev. E **87**, 040102(R) (2013).

[27] A. Pagnani and G. Parisi, Phys. Rev. E **92**, 010101(R) (2015).

[28] K. V. McCloud, M. L. Kurnaz, and J. V. Maher, Phys. Rev. E **56**, 5768 (1997).

[29] T. Vicsek, M. Cserző, and V. K. Horváth, Physica A **167**, 315 (1990).

[30] J. Maunuksela, M. Myllys, O.-P. Kähkönen, J. Timonen, N. Provatas, M. J. Alava, and T. Ala-Nissila, Phys. Rev. Lett. **79**, 1515 (1997).

[31] M. Myllys, J. Maunuksela, M. Alava, T. Ala-Nissila, J. Merikoski, and J. Timonen, Phys. Rev. E **64**, 036101 (2001).

[32] J. De Nardis, M. Medenjak, C. Karrasch, and E. Ilievski, Phys. Rev. Lett. **124**, 210605 (2020).

[33] M. Dupont and J. E. Moore, Phys. Rev. B **101**, 121106(R) (2020).

[34] T. Jin, A. Krajenbrink, and D. Bernard, Phys. Rev. Lett. **125**, 040603 (2020).

[35] Z. Cai, Phys. Rev. Lett. **128**, 050601 (2022).

[36] G. Cecile, J. De Nardis, and E. Ilievski, Phys. Rev. Lett. **132**, 130401 (2024).

[37] D. Squizzato, L. Canet, and A. Minguzzi, Phys. Rev. B **97**, 195453 (2018).

[38] K. Deligiannis, Q. Fontaine, D. Squizzato, M. Richard, S. Ravets, J. Bloch, A. Minguzzi, and L. Canet, Phys. Rev. Res. **4**, 043207 (2022).

[39] Q. Fontaine, D. Squizzato, F. Baboux, I. Amelio, A. Lemaître, M. Morassi, I. Sagnes, L. Le Gratiet, A. Harouri, M. Wouters, I. Carusotto, A. Amo, M. Richard, A. Minguzzi, L. Canet, S. Ravets, and J. Bloch, Nature (London) **608**, 687 (2022).

[40] K. Fujimoto, R. Hamazaki, and Y. Kawaguchi, Phys. Rev. Lett. **127**, 090601 (2021).

[41] K. Fujimoto, R. Hamazaki, and Y. Kawaguchi, Phys. Rev. Lett. **124**, 210604 (2020).

[42] K. Fujimoto, R. Hamazaki, and Y. Kawaguchi, Phys. Rev. Lett. **129**, 110403 (2022).

[43] H. Spohn, J. Stat. Phys. **154**, 1191 (2014).

[44] S. G. Das, A. Dhar, K. Saito, C. B. Mendl, and H. Spohn, Phys. Rev. E **90**, 012124 (2014).

[45] H. Spohn and G. Stoltz, J. Stat. Phys. **160**, 861 (2015).

[46] H. Spohn, *Fluctuating Hydrodynamics Approach to Equilibrium Time Correlations for Anharmonic Chains* (Springer International Publishing, Cham, 2016), pp. 107–158.

[47] R. Ketzmerick, G. Petschel, and T. Geisel, Phys. Rev. Lett. **69**, 695 (1992).

[48] R. Ketzmerick, K. Kruse, S. Kraut, and T. Geisel, Phys. Rev. Lett. **79**, 1959 (1997).

[49] T. Ohtsuki and T. Kawarabayashi, J. Phys. Soc. Jpn. **66**, 314 (1997).

[50] D. J. Luitz, I. Khaymovich, and Y. Bar Lev, SciPost Phys. Core **2**, 006 (2020).

[51] C. Kipnis, C. Marchioro, and E. Presutti, J. Stat. Phys. **27**, 65 (1982).

[52] P. L. Krapivsky and B. Meerson, Phys. Rev. E **86**, 031106 (2012).

[53] E. Bettelheim, N. R. Smith, and B. Meerson, Phys. Rev. Lett. **128**, 130602 (2022).

[54] R. Steinigeweg, H. Wichterich, and J. Gemmer, Europhys. Lett. **88**, 10004 (2009).

[55] Y. Bar Lev, G. Cohen, and D. R. Reichman, Phys. Rev. Lett. **114**, 100601 (2015).

[56] R. Steinigeweg, F. Jin, D. Schmidtke, H. De Raedt, K. Michielsen, and J. Gemmer, Phys. Rev. B **95**, 035155 (2017).

[57] D. J. Luitz and Y. B. Lev, Ann. Phys. (Berl.) **529**, 1600350 (2017).

[58] B. Derrida and A. Gerschenfeld, J. Stat. Phys. **137**, 978 (2009).

[59] S. Ostlund, R. Pandit, D. Rand, H. J. Schellnhuber, and E. D. Siggia, Phys. Rev. Lett. **50**, 1873 (1983).

[60] P. Kalugin, A. Y. Kitaev, and L. Levitov, Zh. Eksp. Teor. Fiz. **91**, 701 (1986).

[61] J. M. Luck and D. Petritis, J. Stat. Phys. **42**, 289 (1986).

[62] M. Kohmoto, B. Sutherland, and C. Tang, Phys. Rev. B **35**, 1020 (1987).

[63] Q. Niu and F. Nori, Phys. Rev. B **42**, 10329 (1990).

[64] H. Hiramoto and S. Abe, J. Phys. Soc. Jpn. **57**, 230 (1988).

[65] F. Piéchon, Phys. Rev. Lett. **76**, 4372 (1996).

[66] V. K. Varma, C. de Mulatier, and M. Žnidarič, Phys. Rev. E **96**, 032130 (2017).

[67] V. K. Varma and M. Žnidarič, Phys. Rev. B **100**, 085105 (2019).

[68] C. Chiaracane, F. Pietracaprina, A. Purkayastha, and J. Goold, Phys. Rev. B **103**, 184205 (2021).

[69] L. J. Vasquez, A. Rodriguez, and R. A. Römer, Phys. Rev. B **78**, 195106 (2008).

[70] A. Rodriguez, L. J. Vasquez, and R. A. Römer, Phys. Rev. B **78**, 195107 (2008).

[71] F. Evers and A. D. Mirlin, Rev. Mod. Phys. **80**, 1355 (2008).

[72] By generating a Fibonacci sequence with $N \gg L$ terms, we can cut out $L+1$ independent samples of of length L. Removing sequences which are related by reflection leads to $\frac{L}{2}$ or $[\frac{L-1}{2}]$ independent configurations for even [odd] number of lattice sites [67,68].

[73] A. Piñeiro Orioli, K. Boguslavski, and J. Berges, Phys. Rev. D **92**, 025041 (2015).

[74] N. Macé, N. Laflorencie, and F. Alet, SciPost Phys. **6**, 050 (2019).

[75] S. Alexander and P. Pincus, Phys. Rev. B **18**, 2011 (1978).

[76] B. Derrida and A. Gerschenfeld, J. Stat. Phys. **136**, 1 (2009).

[77] E. Barkai and R. Silbey, Phys. Rev. E **81**, 041129 (2010).

[78] J. F. Wienand, S. Karch, A. Impertro, C. Schweizer, E. McCulloch, R. Vasseur, S. Gopalakrishnan, M. Aidelsburger, and I. Bloch, arXiv:2306.11457.

[79] S. Aditya and N. Roy, Phys. Rev. B **109**, 035164 (2024).

[80] I. Peschel, J. Phys. A: Math. Gen. **36**, L205 (2003).

[81] I. Peschel and V. Eisler, J. Phys. A: Math. Theor. **42**, 504003 (2009).

[82] I. Klich and L. Levitov, Phys. Rev. Lett. **102**, 100502 (2009).

[83] M. Kiefer-Emmanouilidis, R. Unanyan, J. Sirker, and M. Fleischhauer, SciPost Phys. **8**, 083 (2020).

[84] B. Huckestein, Rev. Mod. Phys. **67**, 357 (1995).

[85] F. Evers, A. Mildenberger, and A. D. Mirlin, Phys. Rev. B **64**, 241303(R) (2001).

[86] A. R. Subramaniam, I. A. Gruzberg, A. W. W. Ludwig, F. Evers, A. Mildenberger, and A. D. Mirlin, Phys. Rev. Lett. **96**, 126802 (2006).

[87] F. Evers, A. Mildenberger, and A. D. Mirlin, Phys. Rev. Lett. **101**, 116803 (2008).

[88] K. S. Tikhonov and A. D. Mirlin, Phys. Rev. B **97**, 214205 (2018).

[89] N. Macé, F. Alet, and N. Laflorencie, Phys. Rev. Lett. **123**, 180601 (2019).

[90] A. Solórzano, L. F. Santos, and E. J. Torres-Herrera, Phys. Rev. Res. **3**, L032030 (2021).

[91] P. W. Anderson, Phys. Rev. **109**, 1492 (1958).

[92] E. Abrahams, P. W. Anderson, D. C. Licciardello, and T. V. Ramakrishnan, Phys. Rev. Lett. **42**, 673 (1979).

[93] P. A. Lee and T. V. Ramakrishnan, Rev. Mod. Phys. **57**, 287 (1985).

[94] B. Kramer and A. MacKinnon, Rep. Prog. Phys. **56**, 1469 (1993).

[95] H. Grussbach and M. Schreiber, Phys. Rev. B **51**, 663 (1995).

[96] J. T. Edwards and D. J. Thouless, J. Phys. C: Solid State Phys. **5**, 807 (1972).

[97] S. Aubry and G. André, Ann. Israel Phys. Soc. **3**, 18 (1980).

[98] S. Roy, I. Khaymovich, A. Das, and R. Moessner, SciPost Phys. **4**, 025 (2018).

[99] X. Deng, S. Ray, S. Sinha, G. V. Shlyapnikov, and L. Santos, Phys. Rev. Lett. **123**, 025301 (2019).

[100] M. Sarkar, R. Ghosh, A. Sen, and K. Sengupta, Phys. Rev. B **103**, 184309 (2021).

[101] D. A. Parshin and H. R. Schober, Phys. Rev. B **57**, 10232 (1998).

[102] E. Cuevas, V. Gasparian, and M. Ortuño, Phys. Rev. Lett. **87**, 056601 (2001).

[103] A. D. Mirlin, Y. V. Fyodorov, F.-M. Dittes, J. Quezada, and T. H. Seligman, Phys. Rev. E **54**, 3221 (1996).

[104] I. Varga and D. Braun, Phys. Rev. B **61**, R11859 (2000).

[105] B. L. Altshuler, E. Cuevas, L. B. Ioffe, and V. E. Kravtsov, Phys. Rev. Lett. **117**, 156601 (2016).